Dalton Transactions

Accepted Manuscript

This article can be cited before page numbers have been issued, to do this please use: H. Li, F. Jiang, G. Zhang, B. Li and L. Wu, *Dalton Trans.*, 2019, DOI: 10.1039/C8DT05146A.

ROYAL SOCIETY OF CHEMISTRY

rsc.li/dalton

ROYAL SOCIETY OF CHEMISTRY View Article Online
DOI: 10.1039/C8DT05146A

Journal Name

ARTICLE

Cyclodextrin-/Photoisomerization- Modulated Assembly and Disassembly of An Azobenzene-Grafted Polyoxometalate Cluster

Hongbo Li, Fengrui Jiang, Guohua Zhang, Bao Li, and Lixin Wu*

Received 00th January 20xx,
Accepted 00th January 20xx

DOI: 10.1039/x0xx00000x

www.rsc.org/

A mono-lacunary Keggin-type polyoxometalate (POM) $[SiW_{11}O_{39}]^{8-}$ grafting an azobenzene group through a Sn ion bridging was prepared and the formed organic-inorganic hybrid cluster was characterized by means of elemental analysis, NMR, TGA, and IR. A vesicular structure of the hybrid cluster assembly in aqueous media was observed in TEM image and it dissociated in the presence of α-/β-, γ- cyclodextrins (α-/β-, γ- CDs) driven by host-guest interaction. The monodispersed inclusion complex further re-assembled into smaller micells under the irradiation of 365 nm light, and this transformation was reversibly controlled by alternating irradiation of 450 nm light. Moreover, in the case of POM-Azo/β-CD system, the re-assembly from monodispersed state to vesicle was also achieved by the addition of a competitive guest molecule. Thus, the reversible host–guest interaction combining reversible photoisomerization of azobenzene group provided multi ways to modulate assembly and disassembly of POM hybrid as well as changes between different assemblies. The present study inspired the potentials of this kind hybrid POMs using in enhanced catalytical reactions and recycles.

Introduction

Self-assembly of colloidal particles and particle like giant molecules displays series of interesting structures and significant functional potentials beyond general small molecules, such as diverse liquid crystalline phases,[1] photonic crystals,[2] template induced self-assemblies for synthesis of porous materials,[3] and so forth. Among those known particles with sizes from micro- to nano-, even smaller scale, polyoxometalates (POMs) represent a type of anionic nanosized inorganic clusters featuring a broad range of precise compositions and uniform multi-topological architectures with rich physicochemical properties,[4] and receive special attentions on their self-assembly studies over the past decades.[5,6] Because the assemblies of these molecular nanoclusters can be used in controlled catalytic reactions,[7] interfacial growth of hybrid catalysts and connecting layers of solar cells,[8,9] it is of importance to understand the assembly and disassembly process in solution systems toward stimulus-response modulation. Liu and his co-workers have firstly demonstrated the formation of "blackberry" structure and assembly process of several naked giant POM clusters versus the change of solvent polarity.[10-13] With the assistance of covalently grafted organic groups and other inorganic clusters, the POMs' assembly becomes easy to be built and modulated via an enhanced hydrophobic force, like those of surfactant enwrapped POM systems.[14-17] The assembled structure of a POM that covalently grafted alkyl chains was also reported to achieve a morphologic alteration between spheres and tubes through electrochemistry controlling to the surface charges of POMs.[18] Though the POM component usually serves as a responsive unit, the operation to the grafting organic group is more favourable when further functionalization of POM clusters is required in their assembled system.[19-23]

Host-guest interaction is widely used in the modulation of self-assemblies of organic molecules by introducing external recognition components because such an interaction can break the original driving force occurred between guest groups or collect the separated building units to aggregate together.[24, 25] Thus, when a suitable guest group is linked to a POM via covalent bond, an additive host molecule can act as the stimuli agent to trigger the interaction change between hybrid POM clusters while the POM's structure property maintains. Following the strategy, to drive the assembly and disassembly of a hybrid POM cluster, we herein report a covalently hybridized Keggin type POM by incorporating a tin ion onto a lacunary silicatungstate as an active site for further modification. Following by grafting a spacer group and utilizing a click reaction, the photoactive azobenzene (Azo) guest group was connected as the end group, affording an organic-inorganic hybrid cluster with formula of $TBA_{0.7}H_{4.3}SiW_{11}O_{39}SnC_{21}H_{23}N_6O$ (POM-Azo, where TBA is tetrabutylammonium). The hybrid POM exhibited amphiphilic behaviour and conducted dynamic assembly structure transformations from vesicular state to a dispersed state via both UV- light irradiation and the host-guest interaction with cyclodextrins (CDs). The reversible change can be also realized by visible light

State Key Laboratory of Supramolecular Structure and Materials, College of Chemistry, Jilin University, Changchun, 130012, China. E-mail: wulx@jlu.edu.cn.

Electronic Supplementary Information (ESI) available: [details of any supplementary information available should be included here]. See DOI: 10.1039/x0xx00000

View Article Online
DOI: 10.1039/C8DT05146A

irradiation, heating, and the addition of another guest molecular component (Scheme 1). Importantly, the present study provides a

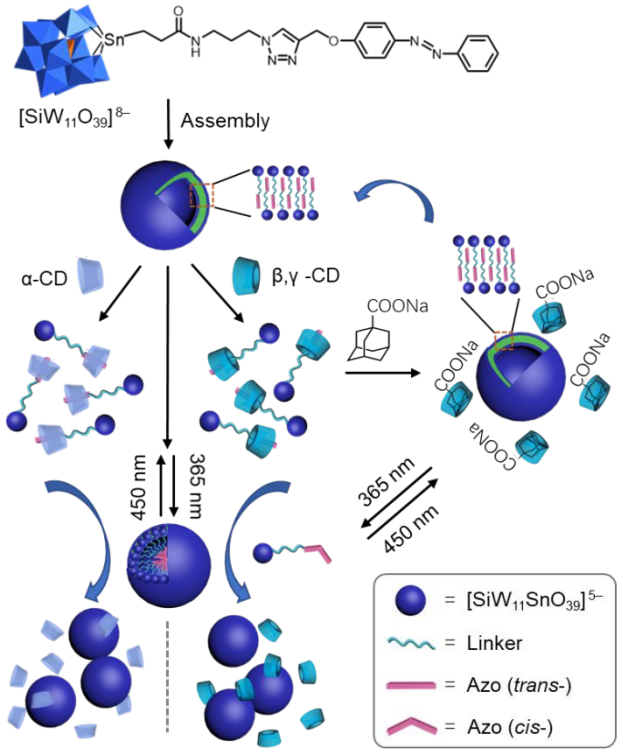

Scheme 1. Schematic formation process of POM-Azo assembly and its controlled transformations to disassembly under the multiple stimulus conditions.

convenient route to modulate the assembly and disassembly of POM cluster particles.

Experimental Section

Materials. Mono-lacunary POM ($K_8SiW_{11}O_{39}$) and initial organic grafting agent $Cl_3Sn(CH_2)_2COOH$ were prepared following the procedures as described elsewhere.[26, 27] All organic agents including α-, β-, and γ- CD, Adamantane-1-carboxylic acid that was used in its sodium salt (Ad-COONa) in neutral condition, and all solvents were obtained from commercial suppliers. Diethyl ether and acetone were dried through distillation over CaH_2. HCl gas was produced by slowly adding concentrated hydrochloric acid to concentrated sulfuric acid upon stirring, dried over concentrated sulfuric acid, and then lead in reactor. All other compounds and solvents were used without further purification. Distilled and deionized water was used in all experiments.

Instruments. Proton nuclear magnetic resonance (^{1}H NMR) spectra were obtained on a Bruker Avance 500 MHz instrument with tetramethylsilane (TMS) as internal reference. Elemental analysis (C, H, N) were conducted on a Vario micro cube, while inorganic elemental analysis for Si, Sn and W was performed on an OPTOMA 3300DV instrument. Thermogravimetric analysis (TGA) was carried out on a Q500 Thermal Analyzer (New Castle TA Instruments) under a flowing air with a heating rate of 10 °C min^{-1}. Fourier Transform Infrared (FT-IR) spectra in pressed KBr pellets were recorded on a Bruker Vertex 80v spectrometer at range of 400 – 4000 cm^{-1} with a resolution of 4 cm^{-1}. The UV-Vis spectra were obtained on a Varian CARY 50 Probe instrument. Dynamic light scattering (DLS) was carried out on a Zetasizer Nano ZS instrument at 25 °C. Circular dichroism spectrum (CDS) was performed on a PMS−450 instrument with a step of 0.5 nm and a resolution of 4 nm s^{-1} in water at 25 °C. Scanning electron microscopic (SEM) images were collected on a JEM-2100F electron microscope with accelerating voltage of 200 KV. Transmission electron microscopic (TEM) images were obtained on a JEOL JEM 2010 without staining. The cryogenic transmission electron microscopy experiment (cryo-TEM) was carried out on a film of solution and moved to a grid under controlled humidity and temperature condition. Excess solution was removed by filter paper and the film was put into liquid ethane quickly in order to freeze with liquid nitrogen. Then images were collected on a JEOL JEM 2010 instrument.

Synthesis of $NH_2(CH_2)_3N_3$. To the doubly distilled water (10 mL) dissolving 3-aminopropanyl bromide (3.28 g, 15.00 mmol) was added sodium azide (3.25 g, 50.00 mmol) dissolving doubly distilled water (15 mL). After 16 h of refluxing, diethyl ether and then potassium hydroxide (4.00 g) was added to the reaction solution under an ice-water bath (lower than 10 °C). Organic phase was separated and then dried over K_2CO_3. The evaporation of organic solvent gives yellowish oily product in yield of 80%. 1H NMR (500 MHz, CD_3CN, 25 °C): δ=1.23 (s, 2H), 1.62 (m, 2H) 2.70 (t, 2H), 3.27 (t, 2H).

Synthesis of $HC{\equiv}CCH_2O(C_{12}H_9N_2)$. The guest molecular component bearing azobenzene group was synthesized according to procedures described in literature.[28] Briefly, to a solution of 4-hydroxyazobenzene (0.50 g, 2.53 mmol) in anhydrous acetone (30 mL) was added K_2CO_3 (1.74 g, 12.61 mmol). After stirring at room temperature for 0.5 h under nitrogen atmosphere, propargyl bromide (1.50 g, 12.61 mmol) was added to the reaction. The mixture was subsequently stirred at room temperature for 24 h. The obtained residue was purified by column chromatography over silica gel (200–300 mesh) with a mixture eluent of petroleum ether/dichloromethane in 5:1 (v/v), giving an orange solid in 91% yield. ^{1}H NMR (500MHz, DMSO-d_6, 25 °C): δ=3.66 (t, 1H), 4.94 (d, 2H), 7.21 (t, 2H), 7.54 (t, 1H), 7.59 (d, 2H), 7.85 (d, 2H), 7.92 (t, 1H). Anal. Calcd for [$C_{15}H_{12}ON_2$, M=236.27]: C 76.25%, H 5.12%, N 11.86%. Found: C 76.55%, H 5.12%, N 11.77%.

Synthesis of $TBA_5[SiW_{11}O_{39}Sn(CH_2)_2COOH]$ (TBA-POM-COOH). Following a similar procedure,[27] to acetonitrile (30 mL) was added $Cl_3Sn(CH_2)_2COOH$ (0.18 g, 0.59 mmol), tetrabutylammonium bromide (1.31 g, 4.06 mmol), and then previously prepared mono-lacunary POM $K_8SiW_{11}O_{39}$. (1.22 g, 0.41 mmol) The mixture was stirred under nitrogen atmosphere for 1.0 h at room temperature. After filtration and evaporation of excess solvent, white solid was obtained. The crude product was dissolved in acetone (5 mL) and ethanol (5 mL), and then precipitated from diethyl ether, giving purified product TBA-POM-COOH as that reported in yield of 68%. ^{1}H NMR (500 MHz, CD3CN, 25°C): δ=1.03 (t, 64H), 1.24 (t, 2H), 1.40 (m, 48H), 1.68 (m,

View Article Online
DOI: 10.1039/C8DT05146A

48H), 2.69 (t, 2H), 3.17 (t, 48H). Anal. Calcd for [$C_{83}H_{185}N_5SiW_{11}O_{41}Sn$, M=4078.4]: C 24.44%, H 4.57%, N 1.72%, Si 0.69%, W 49.58%. Found: C 24.82%, H 4.48%, N 1.75%, Si 0.69%, W 49.68%.

Synthesis of $TBA_5[SiW_{11}O_{39}Sn(CH_2)_2CO]$ (TBA-POM-CO). To conduct the amidation reaction, the above prepared TBA-POM-COOH was firstly transferred into $(TBA)_5[SiW_{11}O_{39}Sn(CH_2)_2CO]$ (TBA-POM-CO). To 10 mL acetonitrile solution of TBA-POM-COOH (500 mg, 0.13 mmol) was added triethylamine (40 µL, 0.14 mmol). After 5 min of stirring to the mixture solution, isobutyl ester of chloroformate (20 µL, 0.16 mmol) was added, and then the solution was stirred under nitrogen atmosphere. Cationic exchange resin and 10 ml of acetone were added to the reaction solution with stirring for another 1.0 h. Oily crude product was obtained after filtration and evaporation of the excess solvent. The purification was performed by dissolving in acetone (3 mL) and dichloromethane (5 mL), and precipitating from diethyl ether (50 mL) with twice of washing with diethyl ether. Dryness in vacuum gives purified intermediate product in yield of 20%. ^{1}H NMR (500 MHz, CD_3CN, 25 °C): δ=1.01 (t, 64H), 1.36 (m, 2H), 1.42 (m, 48H), 1.67 (m, 48H), 2.80 (m, 2H), 3.17 (t, 48H). IR (KBr, cm^{-1}): v=474, 506, 527, 542, 647, 737, 768, 801, 840, 878, 920, 966, 1007, 1211, 1379, 1481, 1729, 2872, 2934, 2961. Anal. Calcd for [$C_{83}H_{184}N_5SiW_{11}O_{40}Sn$, M=4061.4]: C 24.55%, H 4.57%, N 1.72%, Si 0.69%, W 49.79%. Found: C 24.81%, H 4.35%, N 1.75%, Si 0.69%, W 49.78%.

Synthesis of $TBA_5[SiW_{11}O_{39}Sn(CH_2)_2CONH(CH_2)_3N_3]$ (TBA-POM-N_3). The Azo grafting POM complex was synthesized in acetonitrile following the similar procedures described in literature,[27] To the acetonitrile solution (30 mL) of above prepared TBA-POM-CO (1.33 g, 0.34 mmol) was added triethylamine (57 µL, 0.41 mmol) and $NH_2(CH_2)_3N_3$ (127 µL, 1.36 mmol). The mixture solution was stirred overnight. After the addition of cationic exchange resin and acetone (10 mL), the reaction solution was stirred for another 1 h, then filtered. The filtrate was concentrated by rotary evaporation to oily crude product. By adding acetone (7 mL), ethanol (7 mL) and diethyl ether (30 mL) to the purified product was precipitated. Drying in vacuum gives white solid in 84% yield. ^{1}H NMR (500 MHz, CD_3CN, 25 °C): δ=1.01 (t, 60H), 1.19 (m, 2H), 1.43 (m, 40H), 1.67 (t, 40H), 1.81 (m, 2H), 2.65 (m, 2H), 3.19 (t, 40H), 3.30 (m, 2H), 3.42(t, 2H), 6.91 (s, 1H). IR (KBr, cm^{-1}): v=537, 799, 879, 913, 965, 1004, 1064, 1106, 1149, 1348, 1383, 1478, 1541, 1629, 1658, 1726, 2095, 2879, 2939, 2966. Anal. Calcd for [$C_{86}H_{191}N_9SiW_{11}O_{40}Sn$, M=4160.51]: C 24.83%, H 3.63%, N 3.03%, Si 0.68%, W 48.61%, Sn 2.85%. Found: C 24.55%, H 3.65%, N 2.98%, Si 0.69 %, W 48.92%, Sn 2.85%.

Synthesis of $TBA_5[SiW_{11}O_{39}Sn(C_6H_{11}ON)(C_2HN_3)CH_2O(C_{12}H_9N_2)]$ (TBA-POM-Azo). TBA-POM-N_3 (0.83 g, 0.20 mmol) in acetonitrile (5 ml) was mixed with $HC{\equiv}CCH_2O(C_{12}H_9N_2)$ (0.095 g, 0.40 mmol). $CuSO_4{\cdot}5H_2O$ (0.05 g, 0.20 mmol) in 5 mL of water and sodium L-ascorbate (1.59 g, 8.00 mmol) in 5 mL of water were added to the solution, and subsequently, the solution was stirred under nitrogen atmosphere at room temperature for 24 h. Cation-exchange resin and acetone (50 mL) were added to the reaction solution, and then stirred for 1.0 h until the precipitate disappeared. After filtration, the filtrate was evaporated to dryness. The crude product was re-dissolved in acetone (10 mL) upon sonication and then treated with dichloromethane (10 mL) and diethyl ether (120 mL), and the formed precipitate was dried in a vacuum dessicator overnight to give orange solid product in 60% yield. ^{1}H NMR (500 MHz, CD_3CN, 25 °C): δ=1.00 (t, 60H), 1.21 (t, 20H), 1.41 (m, 40H), 1.66 (m, 40H), 2.22 (m, 2H), 2.66 (t, 2H), 3.17 (t, 40H), 3.20 (m, 2H), 4.53 (t, 2H), 5.33 (s, 2H), 7.26 (d, 2H), 7.52 (t, 1H), 7.58 (t, 2H), 7.89 (d, 2H), 7.95 (d, 2H), 8.27 (s, 1H). IR (KBr, cm^{-1}): v=537, 799, 879, 913, 965, 1004, 1064, 1106, 1149, 1348, 1383, 1478, 1541, 1585, 1598, 1632, 1659, 1723, 2879, 2939, 2966. Anal. Calcd for [$C_{101}H_{203}N_{11}SiW_{11}O_{41}Sn$, M=4396.78] C 27.60%, H 4.65%, N 3.50%, Si 0.64%, W 45.99%, Sn 2.70%. Found: C 27.65%, H 4.66%, N 3.42%, Si 0.64%, W 46.31%, Sn 2.70%.

Synthesis of $H_{4.3}TBA_{0.7}[SiW_{11}O_{39}Sn(C_6H_{11}ON)(C_2HN_3)CH_2O(C_{12}H_9N_2)]$ (POM-Azo). POM-Azo was obtained through running TBA-POM-Azo over a silica gel (200–300 mesh) column with CH_3CN as eluent because TBA cations is hard to be exchanged via normal ionic exchange columns. After evaporating excess solvent, the final product exhibiting good solubility in water was obtained as an orange solid in 75% yield. ^{1}H NMR (500 MHz, CD_3CN, 25 °C) : δ=0.92 (t, 2H), 0.94 (t, 8.4H), 1.32 (m, 5.6H), 1.58 (m, 5.6H), 2.03 (m, 2H), 2.36 (t, 2H), 3.07 (m, 2H), 3.17 (t, 5.6H), 4.43 (t, 2H), 5.27 (s, 2H), 7.28 (t, 2H), 7.53 (d, 1H), 7.58 (t, 2H), 7.87 (d, 2H), 7.92 (d, 2H), 7.94 (t, 1H), 8.37 (s, 1H). IR (KBr, cm^{-1}): v=524, 538, 801, 912, 965, 1007, 1146, 1251, 1466, 1499, 1556, 1653, 2876, 2921, 2961. Anal. Calcd for [$C_{32.2}H_{52.5}N_{6.7}SiW_{11}O_{41}Sn$, M=3358.99]: C 11.52%, H 1.58%, N 2.79%, Si 0.84%, W 60.21%, Sn 3.54%. Found: C 11.48%, H 1.61%, N 2.80%, Si 0.84%, W 60.25%, Sn 3.55%.

Sample preparation. Typically, sample solutions (normally 8.4 µM) were prepared at room temperature (25 °C) by dissolving POM-Azo in distilled water and allowed to stand for 15 min to get self-assembly equilibrium. The host-guest interaction was carried out by treating the sample solution with cyclodextrins at a molar ratio of 1:1 and then stirring for 0.5 h. Photo-isomerization experiments were carried out by exposing the sample solution in a quartz cell to a UV light (WHF 203, 8 W, 365 nm) at a distance of 5 cm from light source. The visible light irradiation was performed in a similar way using a 200-W incandescent light source. The samples for TEM were prepared by a drop-casting method on Cu grids, and diluted with a drop of water to get a good assembly dispersion, drying overnight. The sample for SEM was prepared by casting the self-assembly dispersion onto a silicon wafer. After standing for 30 s, the excess solution was removed using a filter paper. The sample preparation for Cryo-TEM was performed with a thin water film on a lacey-supported grid under certain temperature and humidity conditions. The filter paper was used to remove excess solution. The prepared Cu grid was placed in liquid ethane and then in liquid nitrogen. The thin water film on the grid was preserved utilizing a cryotransfer device. Finally, the prepared samples were used for cryo-TEM imaging measurement.

Results and discussion

View Article Online
DOI: 10.1039/C8DT05146A

Characterization and self-assembly of POM-Azo. As shown in Scheme 2, TBA-POM-Azo was synthesized by an initial amidation of 3-aminopropylazide, and then a clik reaction with propargyl

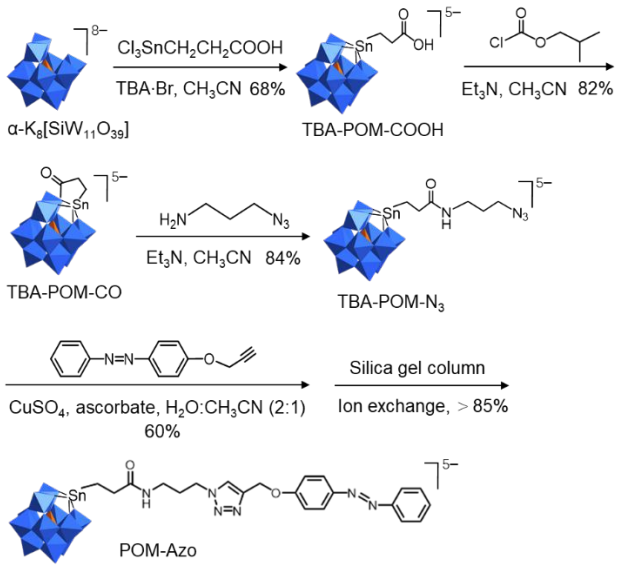

Scheme 2. Detailed synthetic steps of POM-Azo.

azobenzene moiety to an organically grafted lacunary Keggin-type POM, TBA-POM-COOH. To increase the solubility of the hybrid cluster in aqueous media and exclude the influence deriving from counterion, TBA cations were substituted with protons by an ionic exchange reaction over a silica gel though the replacement was still not complete even after three cycles due to the tight binding of TBA. The obtained POM-Azo was characterized by elemental analysis, FT-IR and NMR spectroscopy, and TGA. IR spectrum (Fig. S1) of POM-Azo shows bands at 2876 and 2961 cm^{-1}, which are attributed to methyl and methylene C–H stretching vibrations of residual TBA and organic linker. The peaks at the region of 1500–1700 cm^{-1} are ascribed to amide I and II bands, which partially overlap with the vibration of virgin POM. In addition, the POM-Azo framework is confirmed by the existence of characteristic peaks in the region of 800–1100 cm^{-1}, e.g. 1007 cm^{-1} (Si–O), 965 cm^{-1} (W–O_a), 912 cm^{-1} (W–O_b), and 801 cm^{-1} (W–O_c), where O_a: terminal O atom; O_b: bi-bridging O atom; and O_c: tri-bridging O atom. The ^1H NMR spectrum demonstrates the successful synthesis and purification of POM-Azo and existence of ca. 0.7 of TBA based on the integral of residual peaks (Fig. S2). The TG measurement (Fig. S3) indicates 81.7 wt% remaining of inorganic residual at ca. 470 °C, which is in perfect agreement with calculated 82.2 wt% of inorganic component content as fully oxidized products. The elemental analysis result (Table S1) is also in accordance to the calculated values based on the molecular formula of target chemical composition, further confirming the successful preparation of the hybrid complex. Importantly, both TGA and elemental analysis point to the ratio of inorganic and organic component in POM-Azo.

Even after covalent connection of hydrophobic azobenzene moiety, the ionic substituted POM-Azo maintains soluble in water and performs increased amphiphilic nature. DLS measurement (Fig. 1a) reveals the aggregation of the hybrid cluster with a hydration diameter of ca. 60 nm. The TEM image indicates the spherical assembly and the formation of vesicular like assemblies by casting sample solution onto a copper grid and then sucking with filter paper.

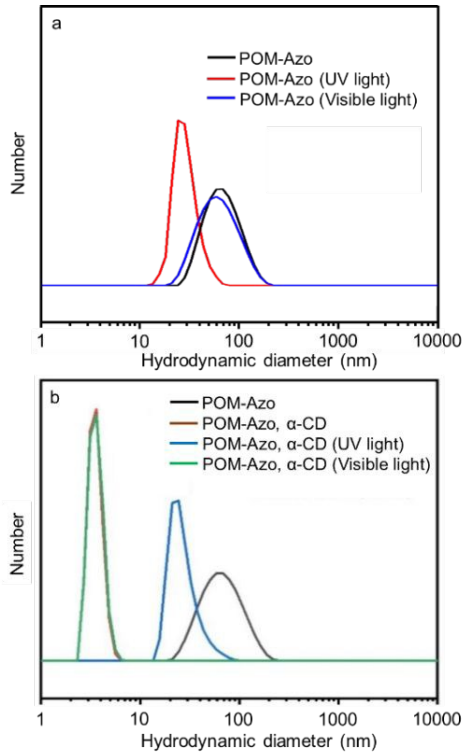

Fig 1. DLS curves of (a) pure POM-Azo in aqueous solution versus the light irradiation, and (b) POM-Azo in inclusion system of α-CD at molar ratio of 1:1 before and after UV-/visible light irradiation for 0.5 h at 25 °C.

The observed layered substructure appears at the edge of self-assembled spheres (Fig. 2a). To exclude the influence from solvent evaporation, Cryo-TEM is carried out for an in-situ measurement to demonstrate the self-assemblies forming in aqueous solution (Fig. 2b). Definitely, we observed spherical assemblies from sample solution with size scale in agreement with those appeared in DLS and dried sample TEM results. As azobenzene group serves as the hydrophobic tail, the amphiphilic nature of the hybrid cluster drives the formation of both aggregation morphology and packing structure in aqueous solution. The ordered aggregation of azobenzene groups can be identified through the change of UV-visible spectrum.[29] In contrast to the absorption band position of azobenzene group in its monodispersed state, ordered aggregation leads to a band shifting in the spectrum because of π-π interaction induced change of electronic energy level. Due to the less effect of host-guest interaction on the electronic state, the absorption band of included azobenzene group is ascribed to the absorption of monodispersed state. Thus, the observed blue shift (from 343 nm to 336 nm) of absorption band (Fig. S4) demonstrates the ordered assembly for POM-Azo alone in aqueous solution and it is rational for the hybrid cluster to form a bilayer structure in the vesicular assemblies.

View Article Online
DOI: 10.1039/C8DT05146A

Modulation of POM-Azo assembly via CD inclusion. Since the azobenzene moiety is known as a typical guest group to have inclusion interaction with some CD hosts, the addition of CDs can be used for the modulation of the self-assemblies of POM-Azo. To

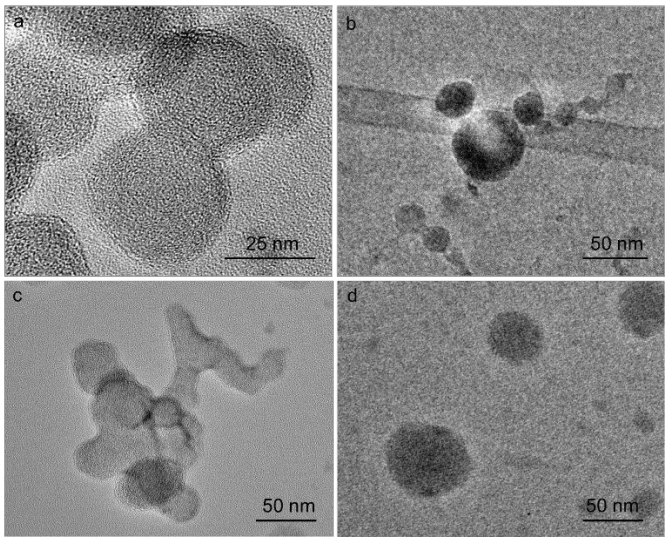

Fig 2. (a) TEM and (b) Cryo-TEM images of POM-Azo in aqueous solution with a concentration of 8.4 μM at 25 °C, and TEM images of the solution after exposing to (c) UV light for 0.5 h and then to (d) visible light for another 0.5 h.

detect the inclusion interaction, aqueous solution of POM-Azo is treated with equimolar amount of α-CD, and the mixture is incubated for 0.5 h at room temperature. It is seen that with the addition of α-CD, the induced Cotton signal of azobenzene group appears and it can be well interpreted to derive from the transfer of inner chirality in CD cavity due to the host-guest interaction (Fig. 3a).[30, 31] In ^{1}H NMR spectrum, chemical shifts sourcing from azobenzene group move larger and broaden after α-CD is added, also confirming the inclusion interaction (Fig. S5). In addition, H–H correlations between POM-Azo (in *trans*- state) and the inner cavity of α-CD are observed in 2D NOESY NMR spectrum of POM-Azo and α-CD mixture solution, further supporting the formation of inclusion complex (Fig. S6). The correlations of protons attributing to H(h) and H(i) from Azo group with the protons H(3) and H(5) deriving from inner cavity also indicate the primary face of α-CD getting into azobenzene firstly. Just like that the assembly of POM-Azo derives from the hydrophobic interaction between organic moiety, the shielding to the hydrophobic interaction triggers a dissociation of the formed assemblies. The inclusion of α-CD isolates azobenzene groups and relieves the hydrophobic interaction among these organic groups. After mixing with α-CD, the observed POM-Azo assemblies dissociate quickly from aggregated state with diameter of ca. 60 nm to a dispersed state with a hydrodynamic diameter of ca. 3.6 nm, as shown in DLS measurement (Fig. 1b). Since this size scale is very close to the inclusion complex comprising of POM-Azo and α-CD, we believed that the inclusion complex becomes its monodispersed state. The characterization of TEM (Fig. 4a and 4b) displays a morphologic consistence, and the observed high contrast domain with size of ca. 1.0 nm supports the mono- dispersion of POM-Azo in the presence of α-CD.

Modulation of POM-Azo assembly via photo-irradiation. While

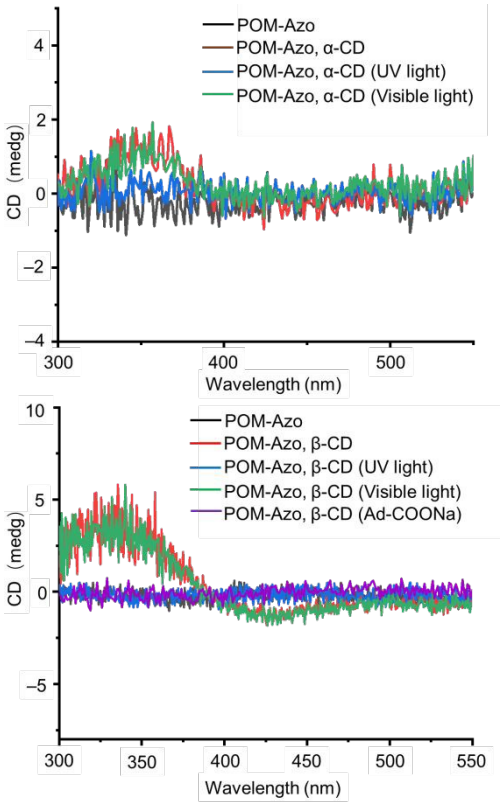

Fig 3. Circular dichroism spectra of POM-azo (black); POM-azo and β-CD with the molar ratio of 1:1 at the initial (red), after UV light irradiation for 0.5 h (blue), and after visible light irradiation for 0.5 h (green); POM-azo, β-CD and Ad-COONa with the molar ratio of 1:1:1.1 (purple) in water at 25 °C.

acting as a guest unit and hydrophobic tail, azobenzene moiety is also a photoactive group exhibiting *trans*- and *cis*- isomerization change, which can be used for the modulation of POM-Azo assemblies.[32, 33] As shown in Fig. S7a, most of *trans*-azobenzene groups of POM-azo transform into *cis*-form upon UV light irradiation and the isomerization equilibrium can be reached in ca. 1.0 min. Based on the calculation of proton integral value in ^{1}H NMR spectra (Fig. S8), the *trans*-to-*cis* conversion efficiency is estimated to be ca. 92% and the efficiency for reverse *cis*-to-*trans* transition is ca. 94% with visible light irradiation of 450 nm in 2 min (Fig. S7b). The reversible transformation from *trans*- to *cis*- transition does not show obvious weakening in five cycles (Fig. S7c and S7d). The conformation of azobenzene group in *cis*- state becomes unfavorable for the tight packing due to increased hydrophilicity and the distorted spatial structure, and thus the light irradiation of 365 nm to the original POM-Azo solution leads to the regular spherical assembly fusing into irregular morphology (Fig. 2c and 2d). Apparently, it is the distorted conformation of azobenzene drives the assembly change. Interestingly, the reverse conformation change of azobenzene group

View Article Online
DOI: 10.1039/C8DT05146A

to the *trans*- state with 450 nm light irradiation promotes the assembly back to the regular spherical morphology, due to linear structure recovering of POM-Azo.

With this property, the photo isomerization of azobenzene group attached in POM is then used for interaction modulation of included

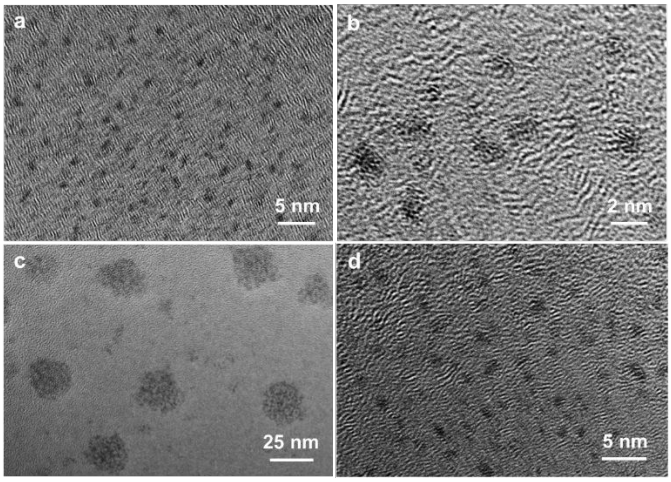

Fig 4. TEM images of POM-Azo solution mixed with α-CD mixture (1:1 molar ratio) at the state (a, and local amplified b) before and (c) after UV light irradiation (365 nm) for 0.5 h, and then (d) visible light irradiation for 0.5 h at 25 °C.

POM-Azo system, where the strong inclusion of POM-Azo with α-CD mainly occurs at the *trans*- state. Accompanying with the illumination of 365 nm light to the POM-Azo solution mixing with α-CD, the transition from isolated inclusion complex to spherical assembly (Fig. 4c and 4d) is observed, which is quite similar to that of POM-Azo alone subjecting to a UV light irradiation. Though the polarity in cis- state becomes high with respect to the trans- state, the azobenzene group is still hydrophobic and tends to decrease interfacial energy by forming assembly. Since the *cis*-isomer of POM-Azo is no longer complexed by α-CD, as a result, the observed assembly of POM-Azo in cis- form in the inclusion system is quite similar to that of POM-Azo alone subjecting to a UV light irradiation. In agreement with TEM observation, the DLS measurement affords a hydrodynamic diameter of the aggregate at ca. 25 nm (Fig. 1b), much smaller than the speculated vesicular assembly in *trans*- state. This assembly can be dissociated reversibly to the isolated state by simply using a visible light irradiation with wavelength of 450 nm and the assembly and disassembly cycles can be also repeated several times through alternate UV and visible light irradiations.

In addition to the UV-visible spectral characterization, the photo isomerization induced dissociation and re-formation of host-guest inclusion are evaluated by induced CDS change (Fig. 3a). After the 365 nm light irradiation to the included POM-Azo system, the induced Cotton signal close to 350 nm disappears completely, which implies the getting out of guest azobenzene group from CD cavity. But the signal re-emerges again after undergoing a 450 nm light irradiation. As the chirality induction only occurs inside the cavity of α-CD, the disappeared Cotton signal clearly demonstrates the discharging of *cis*- azobenzene group from the CD's cavity.

Multiple modulation of POM-Azo assemblies via competitive inclusion. For photo irradiation controlling process, the transformation occurs from the assembly of POM-Azo alone in trans- state to the assembly of POM-Azo in cis- state. In the inclusion system with α-CD, the assembly of POM-Azo is dissociated only in one way while the photoisomerization leads to the transformation from monodispersed POM-Azo in trans- state to the assembly of POM-Azo in cis- state.

To extend the reversible cycle of the stimuli-response and realize a multiple modulation for the self-assemblies of POM-Azo, we use β-CD to repeat the modulation of assembly and disassembly of POM-Azo like that in the presence of α-CD. With the addition of 1:1 molar ratio of β-CD, the cyclodextrin with larger cavity than α-CD, the POM-Azo assembly dissociates following the same behaviors as that occurred in the system containing α-CD, because of the identical inclusion property of the two CDs. Similarly, a well-pronounced chirality signal belonging to azobenzene group is observed in circular dichroism spectrum of mixture aqueous solution containing equimolar POM-Azo (*trans*-) and β-CD (Fig. 3b). The change of chemical shifts also appears in corresponding ^{1}H NMR spectrum (Fig. S9). These results indicate the host-guest interaction between POM-Azo and β-CD, which is further confirmed by the appearance of two cross-correlation peaks between POM-azo (*trans*) and β-CD in 2D NOESY NMR spectrum (Fig. S10). Moreover, the NOESY result demonstrates that the primary face of CD in the inclusion complex locates inside facing to the POM. The TEM observation to the POM-Azo (*trans*- state):β-CD (1:1 molar ratio) mixture solution after encountering a 15 min of sonication and 0.5 h of aging, shows that POM-Azo becomes monodispersed (Fig. 5a). The subsequent UV light (365 nm) irradiation triggers the formation of POM-Azo into micelle like small assemblies as that of POM-Azo and α-CD mixture system due to its transformation of azobenzene group into *cis*- state (Fig. 5b and 5c). The following visible light (450 nm) irradiation to the mixture solution makes the assembly dissociated back to monodispersed inclusion complex (Fig. 5d). The DLS and CDS measurements (Fig. S11 and Fig. 3b) indicate similar mechanism for the transformation cycle between assembly and disassembly. Due to the larger cavity of β-CD than that of α-CD, the formed monodispersed state and the assemblies can be further modulated. When a competitive guest component, Ad-COONa, is added as the modulation agent (1.1 equiv.), its higher binding capability makes it easier replace azobenzene from the inclusion with β-CD quickly. After aging for a while, TEM image shows the reappearance of vesicle like assemblies of POM-Azo (Fig. 6). Because of unloading from β-CD driving by competitive inclusion of Ad-COONa, the free POM-Azo in *trans*- state re-forms the assembly like that of the hybrid cluster alone. The DLS measurement also shows the size increase of complex assembly from ca. 5 nm to ca. 60 nm when adding Ad-COONa into the sample solution, demonstrating the transferring of monodispersed state of included POM-Azo with β-CD to the larger assembly of free POM-Azo in non-included state. Such a competitive inclusion of Ad-COONa can

View Article Online
DOI: 10.1039/C8DT05146A

also be used to the photo isomerization system of POM-Azo with β-CD after encountering a UV light (365 nm) irradiation. When a visible light (450 nm) is used, the assembly of POM-Azo in *cis*- state does not get back to the included state, but instead, forms vesicular assemblies like that of isolated POM-Azo. In agreement with β-CD, γ-CD display a very similar behaviour in modulation the assembly of POM-Azo and competitive inclusion (data not shown) though its inner cavity is a bit larger.

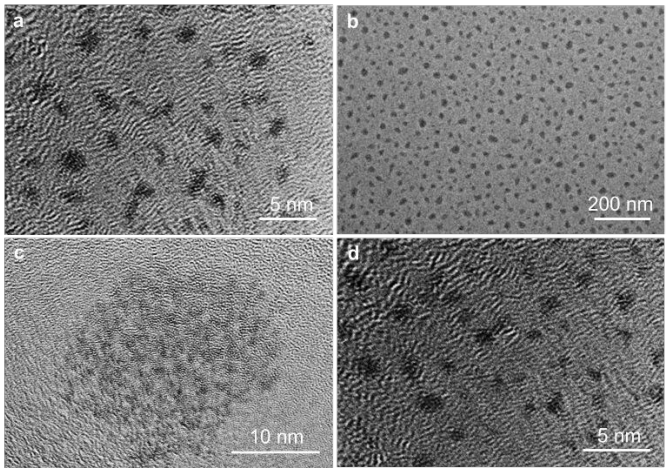

Fig 5. TEM images of (a) inclusion complex of POM-azo and β-CD, (b) the inclusion complex after encountering UV light irradiation (365 nm) to (a) for 0.5 h and (c) the local amplification, and (d) visible light irradiation (450 nm) to (b) for 0.5 h at room temperature (25 °C).

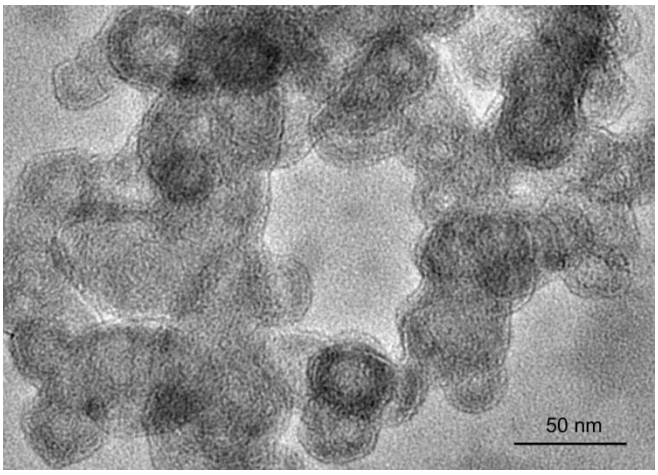

Fig 6. TEM images of POM-azo, β-CD and Ad-COONa with the ratio of 1:1:1.1 in water at 25 °C.

Conclusions

We successfully synthesized an organically grafted inorganic hybrid cluster with photo responsive guest group. The prepared water-soluble compound possessing amphiphilic feature not only displayed general assembly property in aqueous solution, like those hydrophobic group grafting POMs, but also showed dynamic reversible transformations via multiple physical and chemical modulations. In addition to single controlling the assembly through host-guest interaction or light irradiation, the combination of dual controls, together with the competitive inclusion agent, provides rich transformations (Scheme 1) of assembly structure for one POM in solution system. The present results demonstrate that the POM-Azo hybrid cluster could be a multifunctional building block for self-assembled materials. On the other hand, the strategy used in this study can also help in searching effective strategies for controlling the existing state of POMs, which are important for the applicable catalysis in both homogenous and heterogenous systems.

Conflicts of interest

There are no conflicts to declare.

Acknowledgements

The authors acknowledge the financial supports from the National Natural Science Foundation of China (21773090, 21574057), the Changbaishan Distinguished Professor Funding of Jilin Province, and the Program for JLU Science and Technology Innovative Research Team (2017TD-10).

Note and reference

1. W. Li and L. X. Wu, *Polym. Int.*, 2014, **63**, 1750−1764.
2. T. Dasgupta and M. Dijkstra, *Soft matter*, 2018, **14**, 2465−2475.
3. A. Kovalenko, K. Zimny, B. Mascaro, T. Brunet and O. Mondain-Monval, *Soft matter*, 2016, **12**, 5154−5163.
4. M. T. Pope and A. Müller, *Angew. Chem. Int. Ed. Engl.*, 1991, **30**, 34−48.
5. H. Liu, C. H. Hsu, Z. Lin, W. Shan, J. Wang, J. Jiang, M. Huang, B. Lotz, X. Yu, W. B. Zhang, K. Yue and S. Z. Cheng, *J. Am. Chem. Soc.*, 2014, **136**, 10691−10699.
6. B. Li, W. Li, H. L. Li and L. X. Wu, *Acc. Chem. Res.*, 2017, **50**, 1391−1399.
7. Y. Yang, B. Zhang, Y. Z. Wang, L. Yue, W. Li and L. X. Wu, *J. Am. Chem. Soc.*, 2013, **135**, 14500−14503.
8. Y. C. Chen, S. Wang, L. W. Xue, Z. G. Zhang, H. L. Li, L. X. Wu, Y. Wang, F. H. Li, F. L. Zhang and Y. F. Li, *J. Mater. Chem. A*, 2016, **4**, 19189−19196.
9. Y. C. Chen, S. M. Zhang, Q. M. Peng, L. X. Wu, F. H. Li and Y. Wang, *J. Mater. Chem. A*, 2017, **5**, 15294−15301.
10. T. B. Liu, *J. Am. Chem. Soc.*, 2002, **124**, 10942−10943.
11. T. B. Liu, E. Diemann, H. Li, A. W. Dress and A. Müller, *Nature*, 2003, **426**, 59-62.
12. T. B. Liu, *J. Am. Chem. Soc.*, 2003, **125**, 312-313.
13. M. L. Kistler, A. Bhatt, G. Liu, D. Casa and T. B. Liu, *J. Am. Chem. Soc.*, 2007, **129**, 6453−6460.
14. J. Zhang, Y. F. Song, L. Cronin and T. B. Liu, *J. Am. Chem. Soc.*, 2008, **130**, 14408−14409.
15. M. H. Rosnes, C. Musumeci, C. P. Pradeep, J. S. Mathieson, D. L. Long, Y. F. Song, B. Pignataro, R. Cogdell and L. Cronin, *J. Am. Chem. Soc.*, 2010, **132**, 15490−15492.
16. X. S. Hou, G. L. Zhu, L. J. Ren, Z. H. Huang, R. B. Zhang, G. Ungar, L. T. Yan and W. Wang, *J. Am. Chem. Soc.*, 2018, **140**, 1805–1811.
17. H. K. Liu, L. J. Ren, H. Wu, Y. L. Ma, S. Richter, M. Godehardt, C. Kübel and W. Wang, *J. Am. Chem. Soc.*, 2019, **141**, 831–839.

View Article Online
DOI: 10.1039/C8DT05146A

18. S. Landsmann, C. Lizandara-Pueyo and S. Polarz, *J. Am. Chem. Soc.*, 2010, **132**, 5315−5321.
19. T. Auvray, M. P. Santoni, B. Hasenknopf and G. S. Hanan, *Dalton trans.*, 2017, **46**, 10029−10036.
20. Y. Yan, B. Li, Q. Y. He, Z. F. He, H. Ai, H. B. Wang, Z. D. Yin and L. X. Wu, *Soft matter*, 2012, **8**, 1593−1600.
21. Z. F. He, Y. Yan, B. Li, H. Ai, H. B. Wang, H. L. Li and L. X. Wu, *Dalton trans.*, 2012, **41**, 10043−10051.
22. M. P. Santoni, G. S. Hanan and B. Hasenknopf, *Coord. Chem. Rev.*, 2014, **281**, 64−85.
23. T. Zhang, A. Sole-Daura, S. Hostachy, S. Blanchard, C. Paris, Y. Li, J. J. Carbo, J. M. Poblet, A. Proust and G. Guillemot, *J. Am. Chem. Soc.*, 2018, **140**, 14903−14914.
24. D. H. Qu, Q. C. Wang, Q. W. Zhang, X. Ma and H. Tian, *Chem. Rev.*, 2015, **115**, 7543−7588.
25. G. C. Yu, K. C. Jie and F. H. Huang, *Chem. Rev.*, 2015, **115**, 7240−7303.
26. A. Tézé, G. Hervé, R. G. Finke and D. K. Lyon, *Inorg. Synth.*, 1990, **27**, 85−96.
27. A. M. Debela, M. Ortiz, C. K. ÓSullivan, S. Thorimbert and B. Hasenknopf, *Polyhedron*, 2014, **68**, 131−137.
28. J. Z. Li, Z. Zhu, L. Ma, G. X. Chen and Q. F. Li, *Macromolecules*, 2014, **47**, 5739−5748.
29. M. Shimomura, R. Ando and T. Kunitake, *Ber. Bunsenges. Phys. Chem.*, 1983, **87**, 1134−1143.
30. B. Zhang, L. Yue, Y. Wang, Y. Yang and L. X. Wu, *Chem. Commun.*, 2014, **50**, 10823−10826.
31. L. Yue, H. Ai, Y. Yang, W. J. Lu and L. X. Wu, *Chem. Commun.*, 2013, **49**, 9770−9772.
32. C. Dugave and L. Demange, *Chem. Rev.*, 2003, **103**, 2475−2532.
33. R. Breslow and S. D. Dong, *Chem. Rev.*, 1998, **98**, 1997−2012.